

Monitoring of Bone Fracture Healing Using Pulsed Mode Ultrasound

Akram S. Bin Sediq, Hasan Al-Nashash and Nasser Qaddoumi

Department of Electrical Engineering at the American University of Sharjah

Abstract—In this paper, a mathematical model that describes the interaction of a pulsed mode ultrasound waves and a multilayered biological structure is developed. As a special case, the model is applied for quantitative monitoring of fractured bone healing. Four different frequencies are considered. It is found that a transducer operating at 1 MHz has the highest sensitivity to the different phases of callus hardening. On the other hand, a 3 MHz transducer yields the highest sensitivity to the thickness of the callus layer. Thus, using both frequencies might prove to be useful for full quantitative monitoring of the bone healing process.

Index Terms— Ultrasound, Pulsed mode, Bone fracture, Tibia.

I. INTRODUCTION

When a bone is fractured, treatment involves reduction or realignment of the bone, immobilization and restoring function through rehabilitation. The healing process starts when new bone (callus layer) forms and fills in the fractured area to restore the original continuity and solidity. It generally goes through the same series of stages for all fractures: inflammation, soft tissue formation, hard tissue formation, new bone and remodeling [2]. As healing progresses, a soft callus layer forms and begins to harden with time. At a later time stage, the callus layer begins to decay. Consequently, by monitoring the hardening and decay of the callus layer, bone healing stage may be quantitatively estimated. Healing is considered to be complete when the bone is almost identical to its original shape before injury and has regained its normal stiffness and strength. A bone fracture may be diagnosed by many diagnostic imaging tests such as X – Rays, Computed Tomography (CT), Magnetic Resonance Imaging (MRI) or Vibratory devices [3-5]. X – Ray radiation is hazardous and is unsafe for repetitive tests. Moreover, fractures are typically visible on primary radiographs. However, the healing process during the early soft tissue formation stage is difficult to

visualize on radiographs. Furthermore, X-rays can not be used for pregnant women or patients who had a barium contrast media or any medication containing bismuth. MRI tests are long and of high cost and can not be repetitive. The MRI machine itself is prohibitively expensive for small hospitals and therefore, it is not available everywhere. Vibratory devices are mechanical sine wave vibrators that are applied to the fracture site [5]. An electromagnetic shaker is pushed against the skin near the distal end of the bone. A miniature accelerometer captures the response of the bone-prosthesis system to the applied vibrations. If there is no fracture, the bone system behaves linearly and only the excitation frequency will be detected. However, if there is a fracture, the system will behave in a non-linear mode and harmonics will be detected by the accelerometer. Experiments have shown that an excitation frequency between 100 Hz to 200 Hz is well suited to detect fractures. Unfortunately however, vibratory devices suffer from the increased signal damping and locating the resonance frequency especially with obese subjects. Recently, the potential of utilizing Ultrasound was demonstrated as a tool to monitor the healing process of the Tibia using continuous mode ultrasound [6]. In this paper, pulsed mode ultrasound is assumed. A mathematical model that is suited for practical pulsed mode applications is developed. The model is applied to the problem of monitoring of the tibia bone healing process. The paper is organized as follows. Section II presents the theoretical derivation of the mathematical model. Results are presented in section III. Finally, conclusions are drawn in section IV.

II. THEORY

In this model it is assumed that an ultrasound transducer is radiating into an N-layer structure, terminated by an infinite half space. Fig. 1 depicts a 3-layer structure terminated by an infinite half space of any material with acoustic impedance Z_4 . Each layer is characterized by four parameters:

Thickness of the i^{th} layer in (m), d_i
Acoustic impedance of the i^{th} layer in ($\text{kgm}^{-2}\text{s}^{-1}$), Z_i
Velocity of the wave in the i^{th} layer in (ms^{-1}), V_i
Attenuation factor of the i^{th} layer in (dBm^{-1}), α_i

According to the reflection laws of ultrasound waves, waves experience reflection whenever they travel from one medium to another. The ratio of the pressure of the reflected wave to

Manuscript received July, 16, 2006.

A. Bin Sediq is a student with the Department of Electrical Engineering at the American University of Sharjah, P.O.Box 26666, Sharjah, UAE (+971-6-5152935, fax: +971-6-5152979); e-mail: b00007719@aus.edu).

H. Al-Nashash is a Professor with the Department of Electrical Engineering at the American University of Sharjah, P.O.Box 26666, Sharjah, UAE (+971-6-5152935, fax: +971-6-5152979); e-mail: hnashash@aus.edu).

N. Qaddoumi is an Associate Professor with the Department of Electrical Engineering at the American University of Sharjah, P.O.Box 26666, Sharjah, UAE (+971-6-5152935, fax: +971-6-5152933); e-mail: nqaddoumi@aus.edu

the pressure of the incident wave is called the reflection coefficient (Γ_i) and it is given as

$$\Gamma_i = \frac{Z_{i+1} - Z_i}{Z_{i+1} + Z_i},$$

Where Γ_i is the reflection coefficient from the interface between the i^{th} layer and the $(i+1)^{th}$ layer.

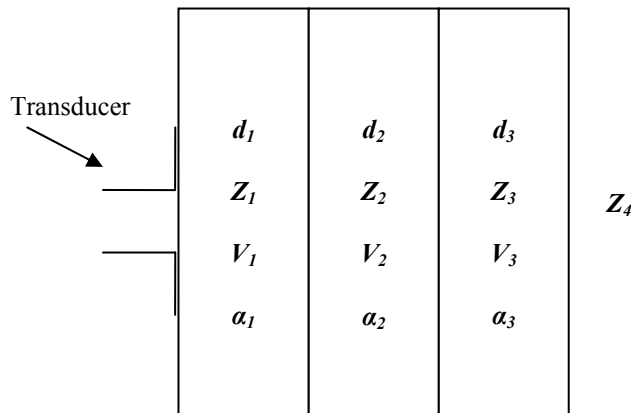


Fig. 1: A 3-layer structure terminated by an infinite half space of a material. Each layer i has thickness d_i , acoustic impedance Z_i , propagation velocity V_i and attenuation factor α_i .

For pulsed mode ultrasound, it is assumed that the incident wave is a delta function at time $t=0$. The wave travels a distance d_1 before reaching the first discontinuity. At the interface, the wave will split into two components: one will propagate to the next layer with amplitude $(1 - \Gamma_1)$ and the other will be reflected and will travel a distance of d_1 to the transducer with amplitude Γ_1 . Therefore, the first reflection which is equal to Γ_1 , will be recorded at the transducer end at

the elapse of time $\frac{2d_1}{V_1}$. The amplitude of the second

reflection is equal to $(1 - \Gamma_1)\Gamma_2(1 + \Gamma_1)$ which will be recorded at the transducer end at the elapse of time $\frac{2d_2}{V_2} + \frac{2d_1}{V_1}$. Finally, the amplitude of the third reflection

is equal to $(1 - \Gamma_1)(1 - \Gamma_2)\Gamma_3(1 + \Gamma_2)(1 + \Gamma_1)$ and will be recorded at time $\frac{2d_3}{V_3} + \frac{2d_2}{V_2} + \frac{2d_1}{V_1}$.

In addition to the main first reflections at each interface, there exists additional multiple reflections within each layer. The first and second multiple reflections and their corresponding times may be obtained in a similar fashion to the main reflections. The first set of multiple reflections appearing at the surface of the transducer occur at:

a) Time $t = \frac{4d_2}{V_2} + \frac{2d_1}{V_1}$ with amplitude

$$(1 - \Gamma_1)\Gamma_2(-\Gamma_1)\Gamma_2(1 + \Gamma_1).$$

b) Time $t = \frac{4d_3}{V_3} + \frac{2d_2}{V_2} + \frac{2d_1}{V_1}$, with amplitude

$$(1 - \Gamma_1)(1 - \Gamma_2)\Gamma_3(-\Gamma_2)\Gamma_3(1 + \Gamma_2)(1 + \Gamma_1).$$

The second set of multiple reflections appearing at the surface of the transducer occur at:

a) Time $t = \frac{6d_2}{V_2} + \frac{2d_1}{V_1}$ with amplitude

$$(1 - \Gamma_1)\Gamma_2(-\Gamma_1)\Gamma_2(-\Gamma_1)\Gamma_2(1 + \Gamma_1)$$

b) time $t = \frac{6d_3}{V_3} + \frac{2d_2}{V_2} + \frac{2d_1}{V_1}$ with amplitude

$$(1 - \Gamma_1)(1 - \Gamma_2)\Gamma_3(-\Gamma_2)\Gamma_3(-\Gamma_2)\Gamma_3(1 + \Gamma_2)(1 + \Gamma_1)$$

Although multiple reflections will continue to take place, usually the first two sets of multiple reflections are of significant amplitude relative to the first reflection. Therefore in this work the first two sets of multiple reflections will be considered.

A unit impulse was assumed to be the input in the derivations outlined earlier. However, to simulate a practical setup, a dying oscillatory pulse with a finite duration should be considered. Hence, the output is obtained by convolving the impulse response with the oscillatory input pulse $f(t)$.

The main and multiple reflections resulting from the structure mentioned earlier show a recursive pattern. Therefore, this is exploited to get a general formula for an N-layer structure. The main reflection in each layer $P_1(i, t)$ and the multiple reflections $P_2(i, t)$ are:

$$P_1(i, t) = [\Gamma_i \prod_{k=1}^{i-1} (1 - \Gamma_k^2) C_{1i}] [\delta(t - \sum_{j=1}^i \frac{2d_j}{V_j}) \otimes f(t)], \quad i = 1..N$$

$$P_2(i, t) = \sum_{m=2}^{\infty} \left[-\Gamma_i^m (\Gamma_{i-1})^{m-1} C_{2im} \prod_{k=1}^{i-1} (1 - \Gamma_k^2) \right] \left[\delta(t - \sum_{j=1}^i \frac{2d_j}{V_j} - \frac{2md_i}{V_i}) \otimes f(t) \right], \quad i = 2..N$$

Where the attenuation coefficients are:

$$C_{1i} = 10^{\frac{-\sum_{j=1}^i 2d_j \alpha_j}{20}} \quad \text{and} \quad C_{2im} = 10^{\frac{-(\sum_{j=1}^i 2d_j \alpha_j + 2md_i \alpha_i)}{20}}$$

III. RESULTS

A. Model Validation

To validate the proposed model, an Aluminum plate immersed in water was used in a laboratory setup. An ultrasound pulser receiver made by OPTTEL was used in conducting an A-scan [7]. The structure parameters are as follows:

- 1st Layer: Water, $Z = 1.5 \times 10^6 \text{ kgm}^{-2} \text{ s}^{-1}$, $d = 1 \text{ cm}$, $V = 1483 \text{ ms}^{-1}$, $\alpha = 0.002 \text{ dBcm}^{-1} \text{ MHz}^{-1}$
- 2nd Layer: Aluminum, $Z = 17 \times 10^6 \text{ kgm}^{-2} \text{ s}^{-1}$, $d = 1 \text{ cm}$, $V = 6320 \text{ ms}^{-1}$, $\alpha = 0.0182 \text{ dBcm}^{-1} \text{ MHz}^{-1}$
- 3rd Layer: Infinite half space of water.

Fig. 2(a) shows the measured incident and reflected voltage as a function of time. The measured signal includes the main and multiple reflections. The first three prominent bursts originate from the transducer, while the rest of the reflections correspond to the main and multiple reflections of the structure. The used measurement system included a time-variable gain amplifier to compensate for the ultrasound wave attenuation as a function of time [7].

The peak of the second burst coincides with the time at which the incident wave leaves the surface of the transducer. Consequently, the first main reflection due to the water aluminum interface appears after 13 μs (it appears at $t \approx 17 \mu\text{s}$). The second main reflection due to the aluminum water interface appears approximately at 20 μs . The obtained results indicate that the measurement system is properly calibrated.

The developed model was tested using the same multi layered structure described above. Fig. 2(b) shows the reflected pressure wave as a function of time. These waves include the main and multiple reflections. The first three bursts are assumed to originate from the transducer with time referenced to the middle of the second burst (to mimic the experimental results) while the rest of the reflections correspond to the main and multiple reflections of the structure. Consequently, the first main reflection due to the water aluminum interface appears after 13 μs (it appears at $t \approx 17 \mu\text{s}$). The second main reflection due to the aluminum

water interface appears approximately at 20 μs . The obtained results reflect good agreement between the model and real measurements. The simulated results show the effect of ultrasound attenuation as a function of time. The time-variable gain amplifier was not included in the simulation.

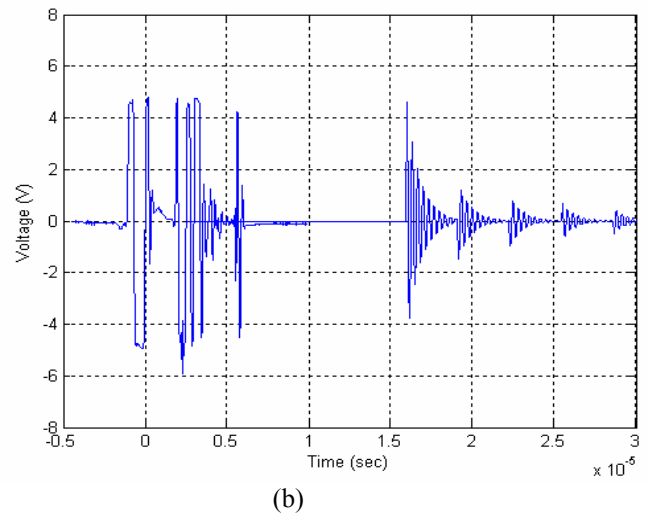
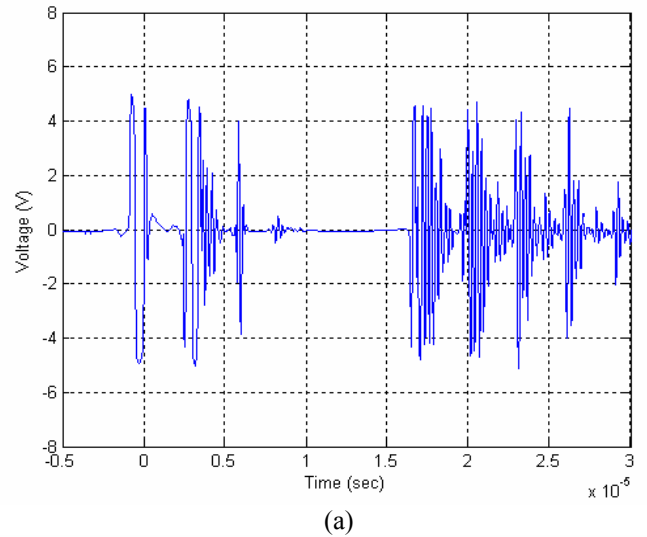


Fig. 2: Pulsed ultrasound A-Scan of a 3-layer structure composed of water-aluminum-water.
a) Experimental b) Simulation.

B. Biological Structure

The model described above was used to model the ultrasound interaction with biological structure composed of skin, fat, callus, and infinite half space of bone as shown in Fig. 1. The structure parameters are as follows:

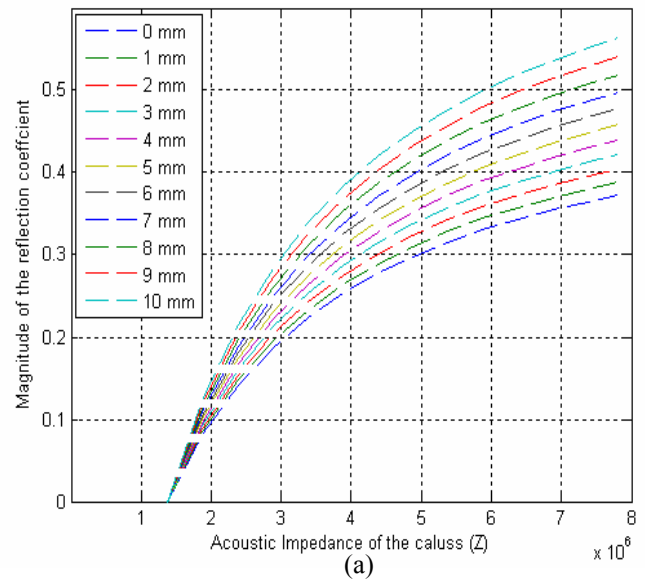
- Layer 1: Delay line of water,
 $Z = 1.5 \times 10^6 \text{ kgm}^{-2} \text{ s}^{-1}$, thickness (d_1) = 6 mm,
Velocity (V_1) = 1483 ms^{-1} , attenuation factor
(α_1) = $0.002 \text{ dBcm}^{-1} \text{ MHz}^{-1}$.
- Layer 2: Skin, $Z = 1.69 \times 10^6 \text{ kgm}^{-2} \text{ s}^{-1}$,
 $d_2 = 2.5 \text{ mm}$, $V_2 = 1537 \text{ ms}^{-1}$, $\alpha_2 =$
 $3.5 \text{ dBcm}^{-1} \text{ MHz}^{-1}$.
- Layer 3: this layer is a fat layer with a thickness (d_3) of 10 mm except for a small circular area (1 cm^2) where the fat is replaced by callus. The fat layer has $Z = 1.38 \times 10^6 \text{ kgm}^{-2} \text{ s}^{-1}$, Velocity = 1450 ms^{-1} , and attenuation = $1.8 \text{ dBcm}^{-1} \text{ MHz}^{-1}$. The callus layer has a thickness of 10 mm with properties similar to fat at the early stages of callus formation. The callus acoustic properties change from those of soft callus (similar to fat) to hard callus (similar to bone). In other words, its acoustic impedance, velocity of the wave and attenuation will increase with time (healing). After the callus hardens, it will begin to decay from 10 mm to 0 mm indicating complete healing. Both the callus thickness and its properties depend on the healing stage. Consequently, monitoring these quantities will reveal information about the healing stage.
- Layer 4: Bone, $Z = 7.8 \times 10^6 \text{ kgm}^{-2} \text{ s}^{-1}$, d_4 is an infinite half-space (usually 3 mm thick), $V_4 = 3500 \text{ ms}^{-1}$, $\alpha_4 = 13 \text{ dBcm}^{-1} \text{ MHz}^{-1}$.

Four different frequencies were considered in the simulation: 1 MHz, 3 MHz, 5 MHz and 10 MHz. Fig. 3 shows the reflection coefficient variation as a function of callus acoustic impedance changes for different callus thicknesses. The simulation results show the remodeling stage of the bone healing process. In Fig. 3a, for example, each curve corresponds to a certain callus thickness starting with soft callus of acoustic impedance similar to fat and ending with hard callus, with acoustic impedance similar to bone. A reflection coefficient of 0.3 represents acoustic impedances ranging between $3 \times 10^6 \text{ kgm}^{-2} \text{ s}^{-1}$ and $5 \times 10^6 \text{ kgm}^{-2} \text{ s}^{-1}$ which is associated with callus thicknesses between 0 to 10 mm. This uncertainty may be resolved using the A-scan which reveals the thicknesses of all layers. Fig. 3b, c, and d show similar results using sensors operating at different frequencies.

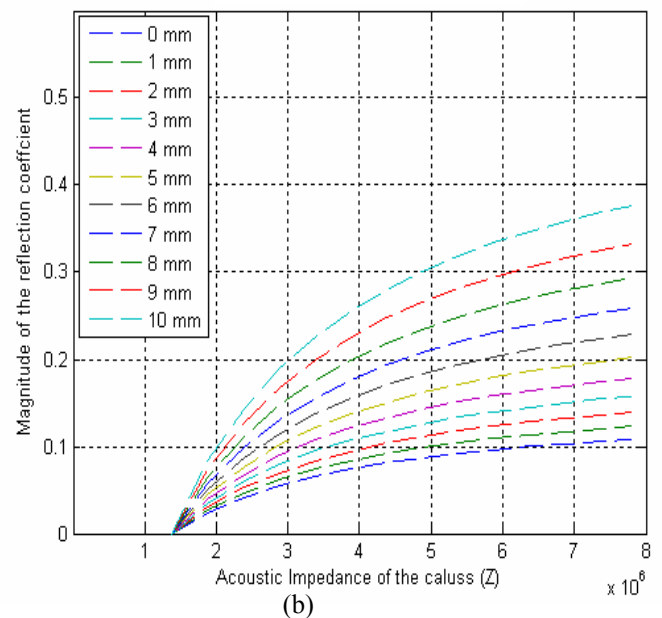
Our criterion to compare the performance of the different transducers is the difference in the magnitude of the

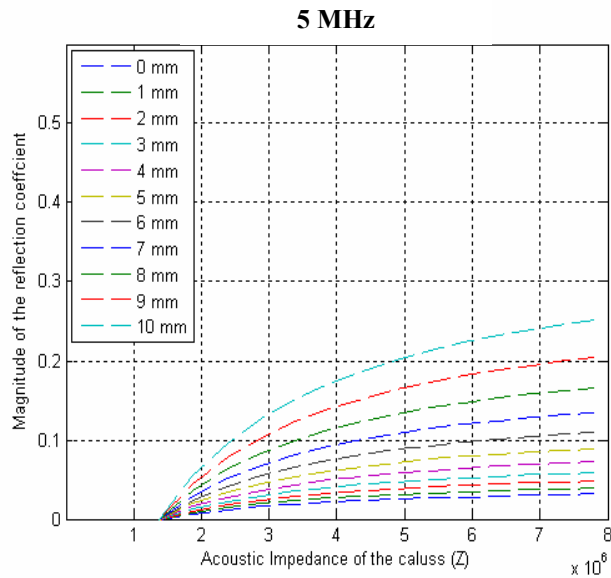
reflection coefficient, which reflects the sensitivity of the transducer to different stages of bone healing. As can be seen, the most sensitive frequency to acoustic impedance, and hence the properties of the callus is 1 MHz since it produces a maximum reflection coefficient difference of 0.55 for callus thickness of 10mm. This difference corresponds to the change from soft callus to hard callus. However, if we target the thickness of the callus, using a 3 MHz sensor was found to be optimum since it produces the maximum difference in the magnitude of the reflection coefficient due to different callus layer thicknesses. This suggests that multi frequency measurements, using 1 MHz and 3 MHz, are needed to reliably determine the status of the callus and its thickness.

1 MHz

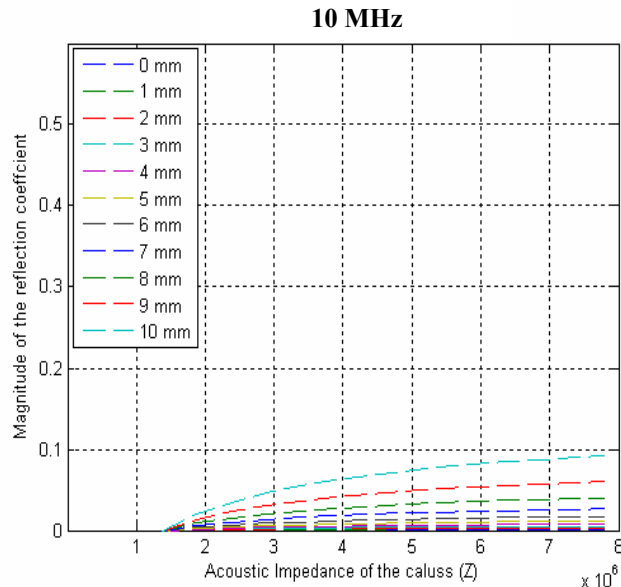


3 MHz





(c)



(d)

Fig. 3: Magnitude of the reflection coefficient as a function of the acoustic impedance of the callus layer at different thicknesses operating at a frequency of a) 1 MHz. b) 3 MHz. c) 5 MHz. d) 10 MHz.

Fig. 4 shows the position of the reflected wave as a function of the thickness of the callus layer. We remark that this measurement parameter is independent of the frequency and the status of the callus, as can be interrupted from the mathematical model. The position of the reflected wave changes linearly with the thickness of the callus. This is extremely important from the practical point of view. It means that quantifying the thickness of the callus is possible due to the linear behavior. Additionally, since different people have different thicknesses of their limb tissues, a shift in time will occur without changing the overall pattern observed in Fig. 4.

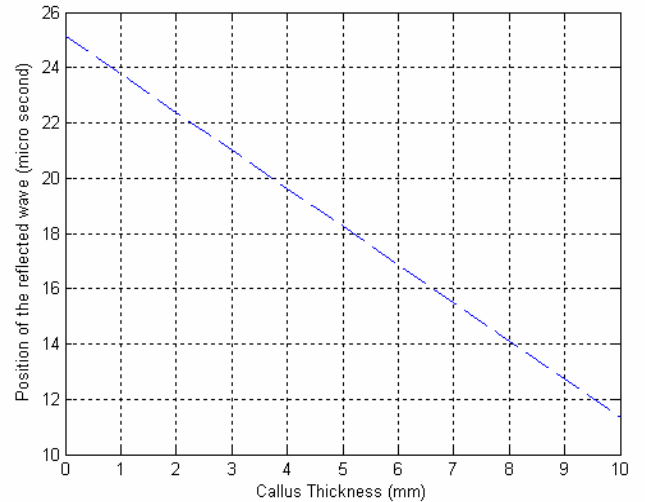


Fig. 4: Position of the reflected wave as a function of the callus thickness.

IV. CONCLUSION

A mathematical model that describes the interaction of ultrasound waves with a multilayer structure was presented. Preliminary experimental results agree with the simulation results. As a special case, the model was applied to monitor bone healing process. A 3-layer structure backed by an infinite half-space was used. Transducers operating at frequencies of 1, 3, 5 and 10 MHz were assumed. Results show that transducers operating at frequencies of 1 MHz and 3 MHz can reliably be used to monitor the bone healing process since they provide highest sensitivity to callus state and thickness.

REFERENCES

- [1] G. Thibodeau and K. Patton, "Anatomy and Physiology," Mosby, 4th edition, 1999.
- [2] R. Johnston, "Problems That Can Occur During Fracture Healing", <http://www.hughston.com/hha/a.fracture.htm>
- [3] A. Webb, "Introduction to Biomedical Imaging", IEEE Press Series and John Wiley and Sons, 2003.
- [4] R. Colier and R. Donarski, "on-invasive method of measuring the resonant frequency of a human tibia in vivo", J Biomed Eng, pp. 9:321–331, 1987.
- [5] R. Collier, R. Donarski, A. Worley and A. Lay. "The use of externally applied mechanical vibrations to assess both fractures and hip prosthesis" Chapter 18, pp. 151-163 in Turner Smith, A.R. (ed.), Micromovement in Orthopaedics. Oxford University Press., 1993.
- [6] A. Hijazy, H. Al – Smoudi, M. Swedan, H. Al – Nashash, N. Qaddoumi, and K.G. Ramesh "Quantitative Monitoring of Bone Healing Process Using Uultrasound," Accepted for publication in the Journal of the Franklin Institute. Available online 15 May 2006.
- [7] OPGUD-01 Pulser & Receiver, <http://www.optel.pl/manual/english/opgud.htm>.